



Effect of PANI addition on structural, optical and electrical characteristics of PVC/Sn_{0.9}Fe_{0.1}S₂ polymer

A. M. El-naggar¹ · Zein K. Heiba² · A. M. Kamal³ · Omar H. Abd-Elkader³ · Mohamed Bakr Mohamed^{2,4}

Received: 17 March 2023 / Accepted: 11 August 2023 / Published online: 13 September 2023
© The Author(s), under exclusive licence to Springer Science+Business Media, LLC, part of Springer Nature 2023

Abstract

Poly (vinyl chloride) (PVC)/Sn_{0.9}Fe_{0.1}S₂/x wt% Polyaniline (PANI) polymers were produced using the solid state reaction method under flows of nitrogen and casting methods. The structure and microstructure characteristics of the Sn_{0.9}Fe_{0.1}S₂ were performed using Rietveld analysis. X-ray diffraction, Fourier transform infrared, Energy dispersive x-ray and scanning electron microscope techniques were used to investigate the constituent elements and surface morphology of the different polymers. The possibility of doping PVC to apply in UV spectra shielding or use as band pass filter for laser protection was investigated. The direct/indirect optical band gaps for PVC (4.94/4.57) eV were reduced to 3.23/1.81 eV as it doped with Sn_{0.9}Fe_{0.1}S₂ and PANI. The impact of PANI and Sn_{0.9}Fe_{0.1}S₂ on the refractive index, extinction coefficient, dielectric parameters, optical conductivity, nonlinear optical parameters and dc conductivity and activation energy of PVC was explored. The fluorescence intensity of PVC was improved as it was loaded with Sn_{0.9}Fe_{0.1}S, and greatly enhanced for PVC/Sn_{0.9}Fe_{0.1}S₂/PANI.

✉ Mohamed Bakr Mohamed
mbm1977@yahoo.com

A. M. El-naggar
elnaggar@ksu.edu.sa

Zein K. Heiba
zein_kh@yahoo.com

A. M. Kamal
amgadmazhar@yahoo.com

Omar H. Abd-Elkader
omabdellkader7@ksu.edu.sa

- ¹ Research Chair of Exploitation of Renewable Energy Applications in Saudi Arabia, Physics and Astronomy Department, College of Science, King Saud University, P.O. Box 2455, 11451 Riyadh, Saudi Arabia
- ² Physics Department, Faculty of Science, Ain Shams University, Cairo, Egypt
- ³ Physics and Astronomy Department, College of Science, King Saud University, P.O. Box 2455, 11451 Riyadh, Saudi Arabia
- ⁴ Physics Department, Faculty of Science, Taibah University, Al-Madina al Munawarah, Saudi Arabia

Keywords PVC · $\text{Sn}_{0.9}\text{Fe}_{0.1}\text{S}_2$ · PANI blend · Structure · Optical · Activation energy

1 Introduction

Organic–inorganic polymer composites attracted much attention owing to the opportunity to achieve desirable physical and chemical characteristics that cover extensive applications in wide sectors for future technologies (Sadek et al. 2021).

PVC is one of the most significant thermoplastic polymers and has wide industrial, agricultural, and medical applications due to its low cost (Mallakpour and Sadaty 2016). Unfortunately, PVC has poor UV stability, which limits its application range (Wang et al. 2022).

The physical properties of different polymers or blended polymers can be improved as long as they are loaded with a suitable dopant. For example, the electrical conductivity of PVC was increased as it was doped with nano ZnO, Fe_2O_3 or TiO_2 (Sadek et al. 2021). Doping PVC with nano ZnTe induced a novel optical feature. Also, its electrical resistivity decreased as the amount of nano ZnTe increased (El-Hachemi et al. 2021a). The photocatalytic investigations reveal the good potential of PVC/nano cadmium sulfide films for MB degradation under UV light irradiation (Rouabah et al. 2021). The adapted thin films of PVC with organosilicon have many uses such as optical stability in electronic applications, low fabrication cost, non-flammability, high heat borne, coating the inner lining of the rocket engine, and heat shielding material (Abed et al. 2022).

PANI is one of the most promising conducting polymers that has redox activity and non-linear optical features. The conductivity of PANI can be adjusted based on its oxidation states and mode of conductivity (Mohamed and Heiba 2017). Higher PANI loading increased the electrical conductivity of the Poly (Ethylene Oxide)/Poly (Vinyl Chloride)/PANI film until the percolation threshold was reached at 10 wt% (Yazid et al. 2017). The polyvinyl alcohol/x wt% PANI blend with 0.25 wt% of PANI revealed the optimal DC conductivity (El-naggar et al. 2023a). The ease way of formation of bismuth vanadate/grapheme oxide/PANI and its excellent performance, could be a promising, competitive and safe visible-light driven photocatalyst in the field of environmental remediation (Biswas et al. 2020). The smart multifunctional devices can be fabricated based on PANI protonated with camphor sulfonic acid—polyethylene oxide doped with nano gallium nitride (Ahmad et al. 2023). The optical features of polyvinyl alcohol (PVA) polymer can be adjusted by adding PANI and nano silver to it (Abdelhamied et al. 2020). The tri-layer polystyrene/PANI/ CeO_2 hybrids shown can be applied in photodegradation towards wastewater containing organic dyes (Chen et al. 2022). The electrical and mechanical characteristics of PVC were enhanced as it was doped with graphene and carbon nanotubes (Taha et al. 2019). Sharma et al. demonstrated that the characteristics of PANI started dominating in PVC/PANI matrix as its amount reached 40 wt%, while minor variations were noticed up to 20 wt% PANI (Sharma et al. 2021). Increasing the content of MWCNTs in the PVC nanocomposite enhanced its thermal stability, dielectric constant and AC conductivity (Abdel-Fattah et al. 2019).

Tin disulfide (SnS_2) has a semiconductor nature, and it can transfer into the intermediate band gap semiconductor materials as it is doped with Fe or V that enables it to absorb more sunlight energy (El-naggar et al. 2022a). Energy harvesting technologies based on polyvinylidene fluoride's (PVDF) piezoelectric properties can greatly benefit from the addition of SnS_2 to the PVDF matrix (Harshvardhan and Singh 2023).

The linear and nonlinear optical properties of PVA/PVP blend were improved as it was loaded with different amounts of nano SnS_2/Fe (El-naggar et al. 2022a). Upon doping a polyvinyl alcohol (PVA)/polyvinyl pyrrolidone (PVP) blend with nano $\text{Sn}_{0.75}\text{M}_{0.25}\text{S}_2$, ($\text{M}=\text{Y}, \text{Fe}, \text{Cr}, \text{V}$) the refractive index value changed in the order $\text{Sn}_{0.75}\text{Cr}_{0.25}\text{S}_2 > \text{Sn}_{0.75}\text{Fe}_{0.25}\text{S}_2 > \text{SnS}_2 > \text{Sn}_{0.75}\text{V}_{0.25}\text{S}_2 > \text{Sn}_{0.75}\text{Y}_{0.25}\text{S}_2 > \text{undoped blend}$ at 600 nm. $\text{Sn}_{0.75}\text{Cr}_{0.25}\text{S}_2/\text{PVA}/\text{PVP}$ blend has the highest dielectric constant. The optical conductivity was improved for all $\text{PVA}/\text{PVP}/\text{Sn}_{0.75}\text{M}_{0.25}\text{S}_2$ blends (Harshvardhan and Singh 2023).

Different procedures were developed to fabricate UV protective materials to reduce the UV irradiation from sun exposure or any other sources to avoid its destructive effects on human health and environment (Wang et al. 2022). Some materials display outstanding UV blocking capability by combining with polymers. For example, the highly dispersed ZnO nanoparticles in PVC films showed UV shielding ability and greatly reduced photocatalytic efficiency (Wang et al. 2022).

In this work, we study the effect of the combination of nano $\text{Sn}_{0.9}\text{Fe}_{0.1}\text{S}_2$ and PANI doping on the structural, morphological, optical, fluorescence and dc conductivity of PVC polymer properties. The possible applications of the formed materials in different fields such as protective materials from different UV types, band pass filters for laser protection, solar cell, photocatalysis, antireflection coatings for solar cells, photonic crystals, and Bragg gratings and optoelectronic applications were also explored.

2 Methods and materials

Nano $\text{Sn}_{0.9}\text{Fe}_{0.1}\text{S}_2$ sample was formed using the solid state reaction method. Stoichiometric amounts from tin (II) chloride dihydrate (Sigma Aldrich, 98%): iron citrate (Sigma Aldrich, 99%): thiourea (Merck, 99%) \equiv 0.9:0.1:4 were mixed and grinded for 3 h then heated at 300 °C (60 min) in a tube electric furnace under flow of nitrogen.

PVC polymer was created using casting method: 2 g of polyvinyl chloride (PVC, Sigma-Aldrich) was dissolved in 40 ml tetrahydrofuran (THF) by a magnet stirrer at room temperature for 4 h, until a clear solution was obtained. $\text{PVC}/\text{Sn}_{0.9}\text{Fe}_{0.1}\text{S}_2$ polymer was formed by repeating the last step but in the present of $\text{Sn}_{0.9}\text{Fe}_{0.1}\text{S}_2$. $\text{PVC}/2 \text{ wt}\% \text{Sn}_{0.9}\text{Fe}_{0.1}\text{S}_2/x \text{ wt}\%$ PANI ($x=0, 0.001, 0.005, 0.01, 0.03, 0.05$) polymers were also produced by repeating the last step but in the presence of PANI (Sigma Aldrich). The formed solutions were poured in Petri dishes for 2 days and the films were formed. The created blended polymers have thickness ≈ 0.28 mm (the digital micrometer).

The x-ray diffraction data were performed using a PANalytical diffractometer (X'Pert MPD, Philips, Cu source, step size: 0.02° , counting time of 10 s/step, 45 kV, 40 mA), the dimensions of the polymer samples are 2 cm \times 1.5 cm. The fluorescence spectra were collected employing a luminescence spectrophotometer (FP-8200 JASCO). Energy dispersive X-ray data (EDS) and scanning electron microscope (SEM) images were conducted using JEOL, Akishima, Tokyo, Japan JED- 2200 Series. The different vibration bands of all polymers were got using a Fourier transform infrared (FTIR) spectroscopy device.

UV diffused reflectance (R), absorbance (A) and transmittance (T) spectra for all samples were obtained using a diffuse reflectance spectrophotometer device (JASCO-V-670) with an attached integrating sphere assembly in the wavelength range of 200–800 nm. The R values were corrected before additional calculations using a similar process as in Ref (El-Naggar et al. 2021).

The optical energy gap (E_g) value of different polymers was obtained using Tauc's relation (El-naggar et al. 2022b):

$$h\nu = D(h\nu - E_g)^r \quad (1)$$

where $h\nu$, D , t and $\alpha (=2.303* A/t)$ are Planck's constant, the frequency of the incident light, a constant known as the disorder parameter, the thickness of the blended polymer and absorption coefficient, respectively. The sort of the transition can be determined by using the value of the parameter r ; $\frac{1}{2}$ for direct allowed and 2 for indirect allowed.

The luminescence (JASCO FP-8200) spectrophotometer under excitation wavelengths of 317 nm was used to obtain the emission from each blend.

The dielectric constant parameters, optical conductivity, energy loss functions, nonlinear optical parameters of the different polymers were derived from the equations in Ref. (El-Naggar et al. 2021).

The electrical conductivity (σ) is given by the following equation using samples in the form of a disk [w1]:

$$\sigma = \frac{L}{R \times A} \quad (2)$$

where L , A , $R(= \frac{V}{I})$, ϵ_0 , V and I are sample thickness (mm), electrode area (m^2), resistance (Ω), permittivity of free space, voltage in volts and current in amperes, respectively.

3 Results and discussion

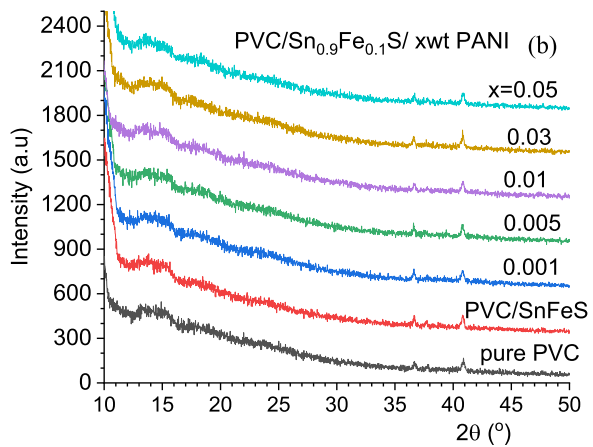
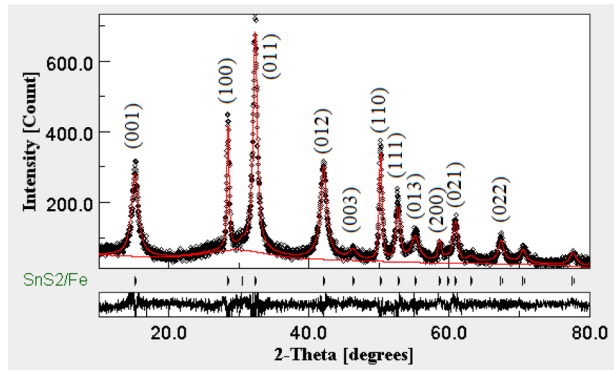
3.1 Structural examination

X-ray diffraction pattern Rietveld analysis was performed for the powder filler $\text{Sn}_{0.9}\text{Fe}_{0.1}\text{S}_2$, Fig. 1a. A single phase of hexagonal brucite structure of space group P-3m1 was determined with cell constants $a = 3.6451(9) \text{ \AA}$ and $c = 5.9564(46) \text{ \AA}$. Anisotropic broadening is obvious, Fig. 1a, for different diffraction lines, implying highly anisotropic crystallite size and microstrain; the determined values are 13.2 nm and 4.8^{-4} along the [001] direction and 2.4 nm and 3.1^{-5} along the [100] direction, respectively

The measured diffraction patterns for pure PVC, PVC/ $\text{Sn}_{0.9}\text{Fe}_{0.1}\text{S}_2$, and PVC/ $\text{Sn}_{0.9}\text{Fe}_{0.1}\text{S}_2/x$ wt% PANI ($x=0.1, 0.5, 1.0, 3.0, 5.0$) are plotted in Fig. 1b. All patterns disclosed the same characteristics as pure PVC pattern and no diffraction peaks for $\text{Sn}_{0.9}\text{Fe}_{0.1}\text{S}_2$ or PANI could be observed owing to the small content of $\text{Sn}_{0.9}\text{Fe}_{0.1}\text{S}_2$ or PANI in the blend. All patterns revealed high diffuse scattering that overlapped with some weak diffraction peaks implying a main amorphous phase of the PVC. The weak diffraction lines at 36.5 and 41° , and the two humps around 15 and 17° are characteristic of PVC which crystallizes in an orthorhombic unit cell of space group Pacm. The poor crystallization of PVC arises from the amorphous nature of atactic and isotactic isomers, and the weak diffraction peaks arise from the crystalline syndiotactic isomer in the polymer (Selvi et al. 2017).

Fourier transform infrared (FT-IR) transmittance data of PVC, PVC/ $\text{Sn}_{0.9}\text{Fe}_{0.1}\text{S}_2$ and PVC/ $\text{Sn}_{0.9}\text{Fe}_{0.1}\text{S}_2/x$ wt % PANI polymers are revealed in Fig. 2. As revealed from the plot, the C-Cl bond stretch, CH rocking and carbonyl group vibrations for PVC polymer appeared at 792, 1146 and $(1731, 1777) \text{ cm}^{-1}$, respectively (Selvi et al. 2017; Brunner 1972; Mallakpour and Shamsaddinimotlagh 2018; Jia et al. 2017). The CH stretching, CH bending and CH rocking vibrations for PVC polymer are located at 2925 and

Fig. 1 **a** Rietveld analysis for $\text{Sn}_{0.9}\text{Fe}_{0.1}\text{S}_2$ and **b** XRD diffraction for PVC, PVC/ $\text{Sn}_{0.9}\text{Fe}_{0.1}\text{S}_2$ and PVC/ $\text{Sn}_{0.9}\text{Fe}_{0.1}\text{S}_2/x$ wt% PANI polymers



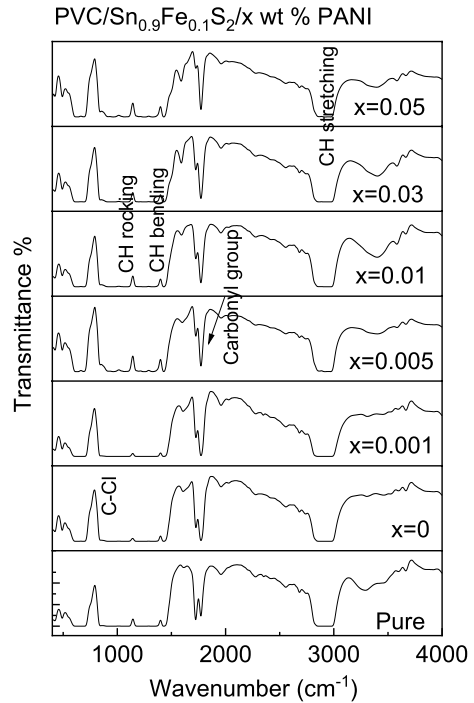
1408 cm^{-1} , respectively (Chen et al. 2017; Soman and Kelkar 2009). Upon doping PVC with $\text{Sn}_{0.9}\text{Fe}_{0.1}\text{S}_2$ and/ or PANI, the positions of the vibration peaks and their intensities changed. For example, the intensities of carbonyl group varied and became one dominant subpeak as the amount of PANI increased in the PVC matrix. The position of C–Cl band changed from 792 cm^{-1} to 800 cm^{-1} as PVC doped with $\text{Sn}_{0.9}\text{Fe}_{0.1}\text{S}_2$ and then reduced to 785 cm^{-1} as the amount of PANI increased in the polymer matrix. This indicated the presence of interaction between PVC and doping materials.

SEM images and EDS analysis for PVC, PVC/ $\text{Sn}_{0.9}\text{Fe}_{0.1}\text{S}_2$ and PVC/ $\text{Sn}_{0.9}\text{Fe}_{0.1}\text{S}_2$ / PANI polymers are shown in Fig. 3. The SEM micrograph of pure PVC is smooth without any pores but with some white patches representing partially immiscibility of PVC polymer. By adding $\text{Sn}_{0.9}\text{Fe}_{0.1}\text{S}_2$ and/ or PANI to the PVC polymer, the surface morphology of the film turns rough. The EDS data of PVC/ $\text{Sn}_{0.9}\text{Fe}_{0.1}\text{S}_2$ and PVC/ $\text{Sn}_{0.9}\text{Fe}_{0.1}\text{S}_2$ / PANI polymers demonstrated the existence of (C, N, Cl), (C, N, Cl, Sn, Fe, S) and (C, N, Cl, Sn, Fe, S) ions in the different polymers, respectively.

3.2 Optoelectronic features

The exploration process for various optical parameters depends on absorption (or transmission) and reflectance data is necessary to understand the variations within the band

Fig. 2 FTIR data for PVC, PVC/Sn_{0.9}Fe_{0.1}S₂ and PVC/Sn_{0.9}Fe_{0.1}S₂/x wt% PANI polymers



gap range. The diffused optical absorption data for PVC, PVC/2 wt% SnFeS and PVC/2 wt% Sn_{0.9}Fe_{0.1}S₂/x wt% PANI polymers have been measured in the wavelength region 200–800 nm, Fig. 4. The absorbance of PVC has two absorption peaks at 214 and 282 nm which are assigned as the electron transfer from $\pi \rightarrow \pi^*$ and $n \rightarrow \pi^*$ transitions owing to (C=C) unsaturated bonds and C–Cl bond, respectively (Rajendran et al. 2007). Upon doping PVC with nano Sn_{0.9}Fe_{0.1}S₂, the absorption increased. This increase is associated with the absorption feature of Sn_{0.9}Fe_{0.1}S₂ sample. Besides, the absorption data exhibited two more extra absorption peaks as PVC/Sn_{0.9}Fe_{0.1}S₂ loaded with different amounts of PANI. These two peaks, located at around 325 and 605 nm, represent the $\pi\text{-}\pi^*$ transition (benzenoid and quinoid units) and polaron band, respectively (Gaabou 2021; Mirmohseni and Wallace 2003). Furthermore, the absorbance spectra of the system increased as the amount of PANI increased. Similar results were observed for PVC doped with MWCNTs and PVA doped with nano Ag and PANI (Abdelhamied et al. 2020; Abdel-Fattah et al. 2019). Also, the plot revealed that loaded blends with PANI above $x = 0.001$ have a good absorbance of UV light at 320 nm (UVA) relative to other samples. In addition, the transmittance data for PVC exhibited approximately 90% over the wavelength range larger than 300 nm, Fig. 5a. The transmittance was reduced to 35–60% as it was loaded with TiO₂. The transmittance was reduced further as the polymer doped with PANI reached zero value as the PANI became higher than 0.003 wt% (opaque material). Samples with $x = 0.005$ and 0.01 exhibited a band pass filter for laser protection. In the visible range, the reflectance of doped PVC polymer increased irregularly as compared with pure PVC, Fig. 5b. Previously, it was found that the absorption and reflectance spectra of PVA/x wt% PANI were raised while transmittance decreased as the amount of PANI increased (Laourari et al. 2022).

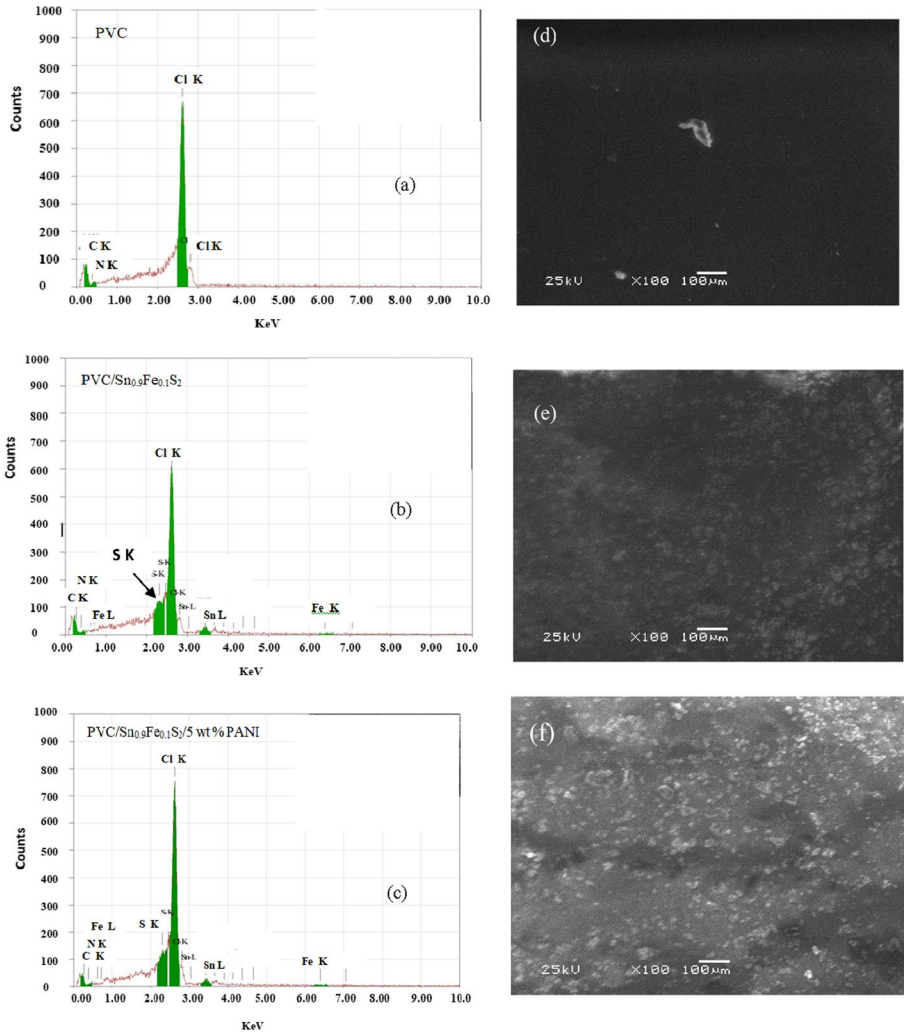


Fig. 3 a–c EDX analysis and d–f corresponding SEM images for PVC, PVC/Sn_{0.9}Fe_{0.1}S₂ and PVC/Sn_{0.9}Fe_{0.1}S₂/PANI polymers

The optical band gap energy (E_g) between the highest occupied molecular orbital (HOMO) and the lowest unoccupied molecular orbital (LUMO) for the different samples can be obtained by analyzing the absorption data near the absorption edge. The direct and indirect optical band gap values for all polymers can be determined using Tauc's formula (Eq. 1) via plotting the graph between $(ah\nu)^2$ or $(ah\nu)^{0.5}$ and the photon energy ($h\nu$) as demonstrated in Fig. 6. The direct and indirect optical band gap values were obtained by extrapolating the linear portion of the curves to zero absorption values. As revealed from the plot, the direct/indirect optical band gap for PVC is 4.94/4.57 eV. These values were decreased to 4.55/3.41 eV as PVC loaded with Sn_{0.9}Fe_{0.1}S₂ and reduced further to (4.45, 3.34, 3.25, 3.26 and 3.23)/(3.03, 1.81, 2.33, 2.56 and 2.47) eV as the amount of x wt % PANI in the polymers became 0.001, 0.005, 0.01, 0.01 and 0.05, respectively. Similar

Fig. 4 Absorbance spectra for PVC, PVC/Sn_{0.9}Fe_{0.1}S₂ and PVC/Sn_{0.9}Fe_{0.1}S₂/x wt% PANI polymers

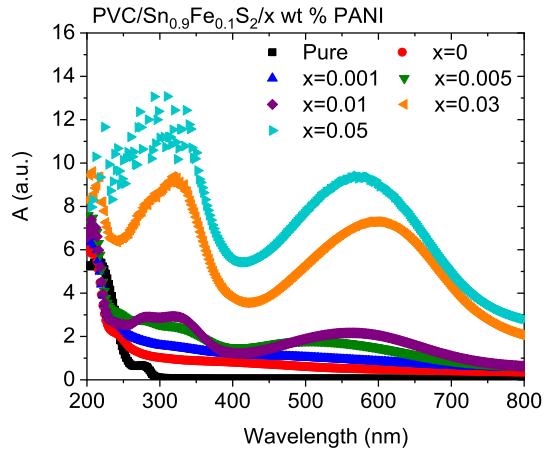
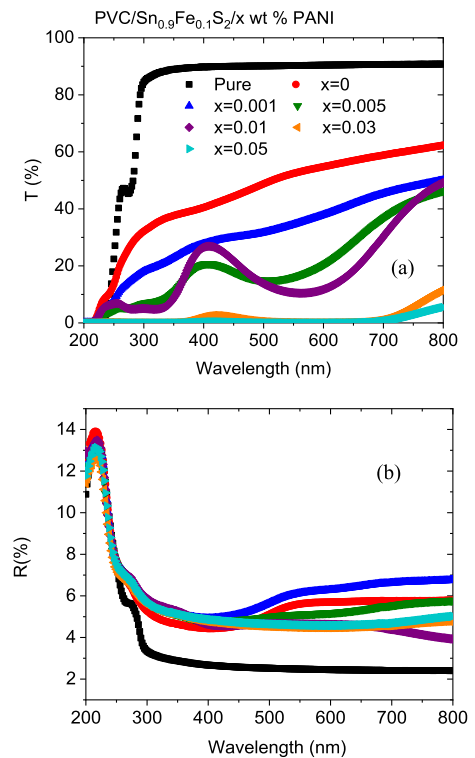


Fig. 5 a Transmittance and **b** reflectance spectra for PVC, PVC/Sn_{0.9}Fe_{0.1}S₂ and PVC/Sn_{0.9}Fe_{0.1}S₂/x wt% PANI polymers



behavior occurred when PVC was doped with NiO, or functionalized graphene oxide or CdS (Rouabah et al. 2021; Taha et al. 2019; Mansour et al. 2015). The decrease in optical band gap may result from the formation of localized states inside the optical band gap of the PVC due to increasing the number of disorders (defects) upon filling with Sn_{0.9}Fe_{0.1}S₂ and different amounts of PANI. Therefore, the investigated doped polymers can be used in solar cells, photocatalysis and optoelectronic applications (Taha 2018).

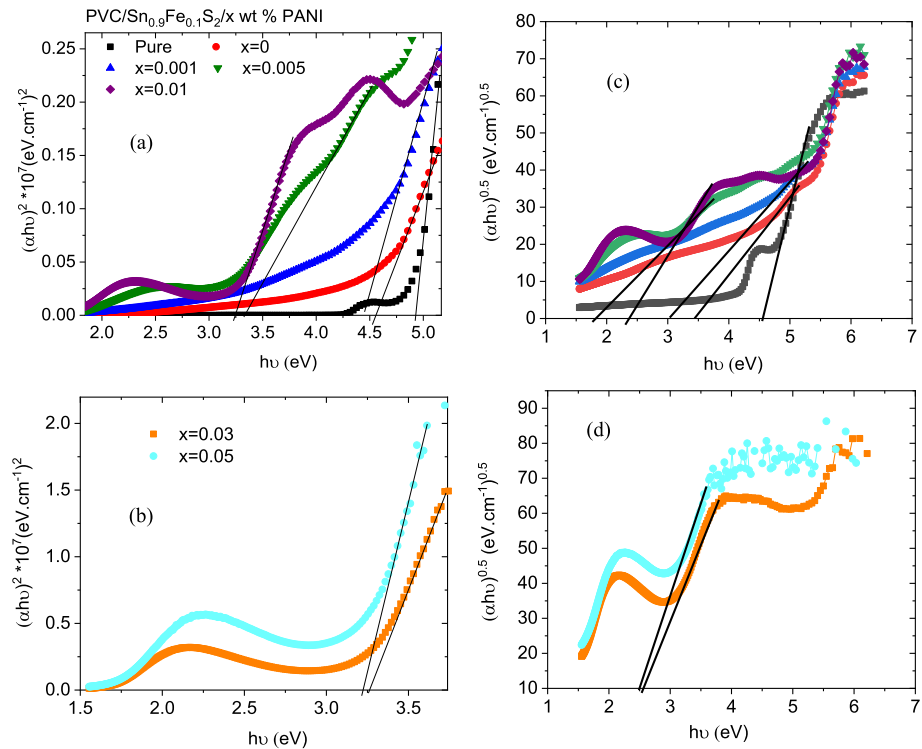
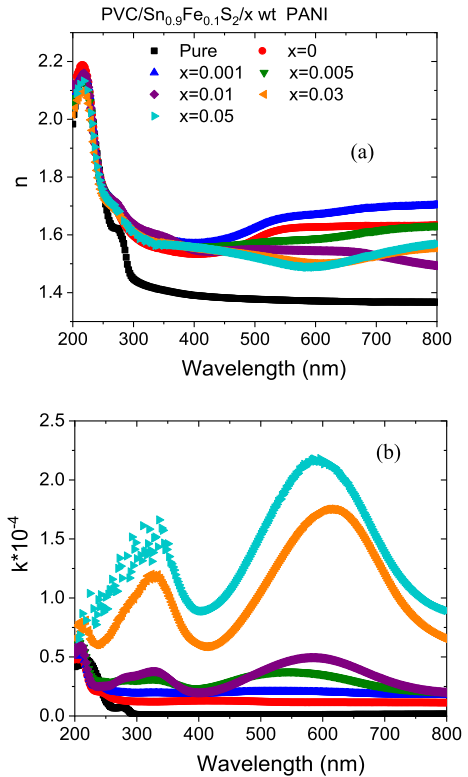


Fig. 6 Tauc relation for **a, b** direct and **c, d** indirect optical transitions for PVC, PVC/Sn_{0.9}Fe_{0.1}S₂ and PVC/Sn_{0.9}Fe_{0.1}S₂/x wt% PANI polymers

The changes in the refractive index (n) values with the wavelength of the incident photons under the effect of doping are very essential parameters for the design of electronic and optoelectronic devices. The extinction coefficient (k) is an optical parameter that reflects the variations taking place during the absorption process within the material. The wavelength dependence of n and k for all samples is shown in Fig. 7a, b, respectively. The n value of PVC increased as it was doped with Sn_{0.9}Fe_{0.1}S₂ and it increased further as it was doped with 0.001 wt % PANI, but with increasing the amount of PANI, the n value reduced. This variation is clear evidence for the polymer matrix intermolecular changes, change in internal strain and aggregation of the material (Abdelhamied et al. 2020; Wadatar and Waghuley 2021; Sayed and Soliman 2000). Such improvement in the values of n enables the doped polymers to be suggested as antireflection coatings for solar cells, photonic crystals, and Bragg gratings (Kroschwitz 1988). On the contrary, the n values of PVA were reduced as it was doped with nano Ag and/or PANI (Abdelhamied et al. 2020). Furthermore, polymer with 0.001 wt% PANI displayed the maximum values of n among the other polymers. Also, the k values rose as PVC doped with Sn_{0.9}Fe_{0.1}S₂ and increased further as the content of PANI raised in the matrix, which may explain the high absorption coefficient. The estimation process for polymers in electronic and optoelectronic applications is dependent on their dielectric constant characteristics. The dielectric constant is one of the essential parameters that describe the polymer's performance. The real part of the dielectric constant (ϵ_r) points to the dispersion mechanism inside the polymer and it

Fig. 7 Spectra variations of **a** refractive index and **b** extinction coefficient with the wavelength for PVC, PVC/Sn_{0.9}Fe_{0.1}S₂ and PVC/Sn_{0.9}Fe_{0.1}S₂/x wt% PANI polymers



illustrates the change in speed of the incident electromagnetic beam by the polarizability influence of the molecules. The imaginary part of the dielectric constant (ϵ_i) gives information about the loss in the incident electromagnetic energy by the medium i.e., it reveals the material resistance to the incident beam of photons. Furthermore, the rate by which the resulting fast electrons can lose energy within the bulk material relates to the volume energy loss function (VELF) while the rate by which electron energy can be lost by the surface of the material is linked to the surface energy loss function (SELF). The variations of the ϵ_r , ϵ_i , VELF and SELF as functions of the wavelength of the incident photon for PVC, PVC/Sn_{0.9}Fe_{0.1}S₂ and PVC/Sn_{0.9}Fe_{0.1}S₂/x wt% PANI polymers are displayed in Fig. 8. As depicted from the graph, both ϵ_r and VELF have higher values than the corresponding ϵ_i and SELF values in each polymer, respectively. ϵ_r revealed a gradual reduction with the wavelength. ϵ_i displayed a gradual reduction with increase in the wavelength for PVC and PVC/Sn_{0.9}Fe_{0.1}S₂ samples. Upon doping PVC/Sn_{0.9}Fe_{0.1}S₂ with PANI exhibited a variable behavior depending on the measured wavelength range. The values of ϵ_r , ϵ_i , VELF and SELF of PVC were increased as it doped with Sn_{0.9}Fe_{0.1}S₂ and/or PANI. As PVA doped with nano Ag and PANI, ϵ_r was reduced while ϵ_i was increased (Abdelhamied et al. 2020). Besides, in the visible range, sample with $x=0.001$ has a higher ϵ_r value. A sample with $x=0.05$ has higher ϵ_i , VELF and SELF values. The variations in ϵ_r and ϵ_i values may result from the change in the absorption coefficient and scattering process, respectively. Besides, these modifications in the real part of the dielectric constant are linked to the variation in the band structure of the PVC polymer, as more states are created within the forbidden gap.

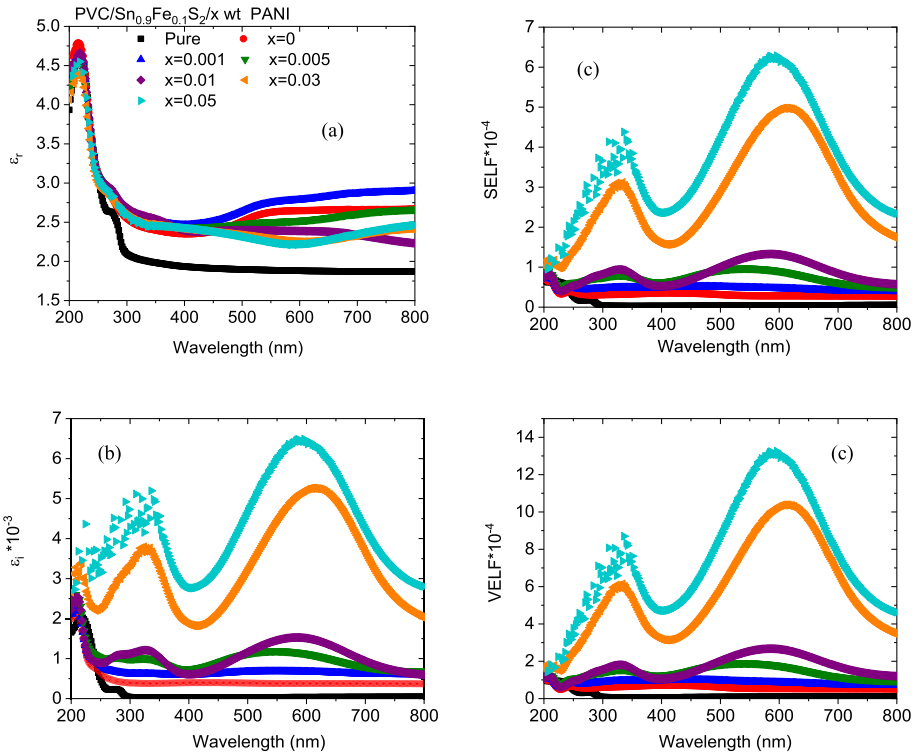
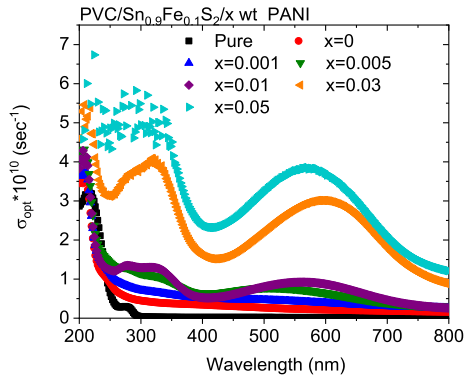


Fig. 8 The changing of **a** real and **b** imaginary dielectric constant, **c** SELF and **d** VELF with the wavelength for PVC, PVC/Sn_{0.9}Fe_{0.1}S₂ and PVC/Sn_{0.9}Fe_{0.1}S₂/x wt % PANI polymers

Additionally, the high values of dielectric loss relate to the modification in the polarization of the host PVC as it doped with filler materials (Ahmed et al. 2021). Moreover, the increase in the values of the SELF and VELF functions with doping PVC with Sn_{0.9}Fe_{0.1}S₂ and/or PANI confirms the presence of higher number of fast electrons. The optical conductivity (σ_{opt}) is a necessary parameter for electronic and optoelectronic device applications. It gives us information about electronic transitions within states. The spectral values of σ_{opt} for PVC and PVC/Sn_{0.9}Fe_{0.1}S₂ polymers illustrated a reduction while the σ_{opt} for polymers doped with PANI exhibited a fluctuation with increasing the wavelength which is similar to the absorbance behavior. The value of σ_{opt} for PVC polymer was increased as it loaded with Sn_{0.9}Fe_{0.1}S₂ and increased further as it doped with different amount of PANI. Similar behavior was detected as PVC loaded with different NiO amounts (Taha et al. 2019). This enhancement in σ_{opt} can be returned to the highly number of free electrons produced by doping effect and therefore increased the number of defect states or disorders within the host PVC matrix which facilitate the movement of electrons within the band gap and hence raised σ_{opt} (Ahmed et al. 2021). Similar results were observed for PVA doped with nano silver and PANI (Abdelhamied et al. 2020). This supports the good miscibility between PANI, nano Sn_{0.9}Fe_{0.1}S₂ and PVC chains as revealed in the XRD data. The spectra dependent on the first-order optical susceptibility ($\chi^{(1)}$), third-order nonlinear susceptibility ($\chi^{(3)}$) and nonlinear refractive index (n_2) for PVC, PVC/Sn_{0.9}Fe_{0.1}S₂ and PVC/Sn_{0.9}Fe_{0.1}S₂/x wt% PANI polymers with the wavelength are displayed in Fig. 9. As depicted from figure, the

Fig. 9 Optical conductivity for PVC, PVC/Sn_{0.9}Fe_{0.1}S₂ and PVC/Sn_{0.9}Fe_{0.1}S₂/x wt% PANI polymers



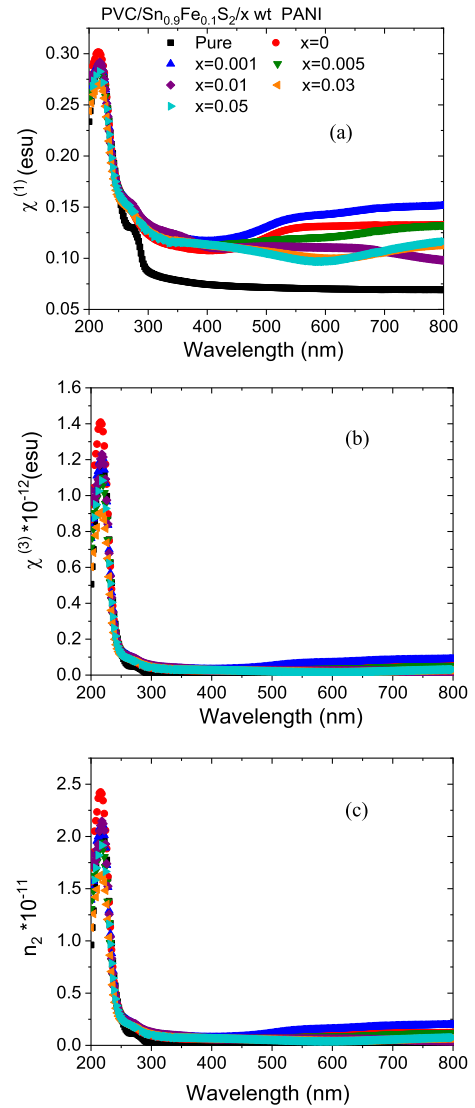
three nonlinear optical (NLO) parameters for PVC polymer were raised as it was doped with Sn_{0.9}Fe_{0.1}S₂ and/or PANI. As the amounts of PANI increased, the increase in NLO parameters are irregularly and their reached maximum values as the ratio of PANI became 0.001, Fig. 10. The NLO parameters of PVC were increased as it was loaded with different contents of NiO (Taha et al. 2019). The obtained results may result from the dependence of the NLO parameter on the n values of the different polymers. The development in the NLO of doped PVC with Sn_{0.9}Fe_{0.1}S₂ and/or PANI is considered a helpful guide for upcoming optoelectronic applications.

3.3 Fluorescence (FL) characteristics

The FL emission spectra of pristine PVC, PVC/Sn_{0.9}Fe_{0.1}S and PVC/Sn_{0.9}Fe_{0.1}S₂/ x wt% PANI, under excitation with $\lambda=317$ nm, are given in Fig. 11a. The spectra exhibited a broad fluorescence emission ranging from 300 to 620 nm with peak intensities depending on the doping ratio (x). The spectra comprise peaks at 346 (near UV), 420 (yellow) with a right shoulder 375–400 nm, 581 nm (orange) and 610 nm with a plateau from 350 to 420 nm. It is expected that the emission from the PVC polymer is dominated by excimer fluorescence (El-naggar et al. 2023b). FL emission spectra of neat PVC film revealed a peak at 380 nm when excited with $\lambda=310$ nm, and the peak was shifted to ~ 425 nm under excitation of 360 nm (Graeme 1985). Under 415 nm excitation wavelength (Rouabah et al. 2021), the FL spectrum of PVC polymer exhibited a strong emission band at 467 nm (blue) related to PVC excimer fluorescence and corresponding to $\pi^*-\pi$ transition. The spectrum conveyed two shoulder bands around 480 and 492 nm, attributed to trapped energy levels generated by impurities in the PVC (El-Hachemi et al. 2021a). For pristine PVC and under excitation of 340 nm, Taha et al. (Ahmed et al. 2021) recorded a wide hump-like emission band that peaked at 401.5 nm (violet).

The FL intensity for the pristine PVC is very weak, Fig. 11b, which was enhanced when PVC was loaded by Sn_{0.9}Fe_{0.1}S, and greatly enhanced as PVC doped with Sn_{0.9}Fe_{0.1}S₂ and PANI. The increase in FL intensity is not linear with PANI percent (Fig. 11b), the intensity greatly increased for $x=0.001$, then decreased for further increases in amount of PANI, probably due to concentration quenching, but is always higher than that of pure PVC. The interactions of PVC and PANI side chains or main chains lead to variations in efficiency of luminescence and temporal evolution (Sharma et al. 2021). The enhancement of luminescence intensity could be attributed to the crosslink-enhanced emission effect between PVC and PANI

Fig. 10 a–c Wavelength dependent of the nonlinear optical parameters for PVC, PVC/Sn_{0.9}Fe_{0.1}S₂ and PVC/Sn_{0.9}Fe_{0.1}S₂/x wt% PANI polymers



(Taha et al. 2020). A similar enhancement in PVC fluorescence intensity was obtained upon loading with CdS (Tao et al. 2020) or with CdTe (Rouabah et al. 2021). Ramazanov et al. (El-Hachemi et al. 2021b) investigated loading PVC with different percents of TiO₂ (1.0, 3.0, 5.0, 10.0%); under excitation wavelength 410 nm, the PL intensity increased with increasing the TiO₂ content up to 5% and interpreted to be mainly due to the growth in the luminescent center surface area.

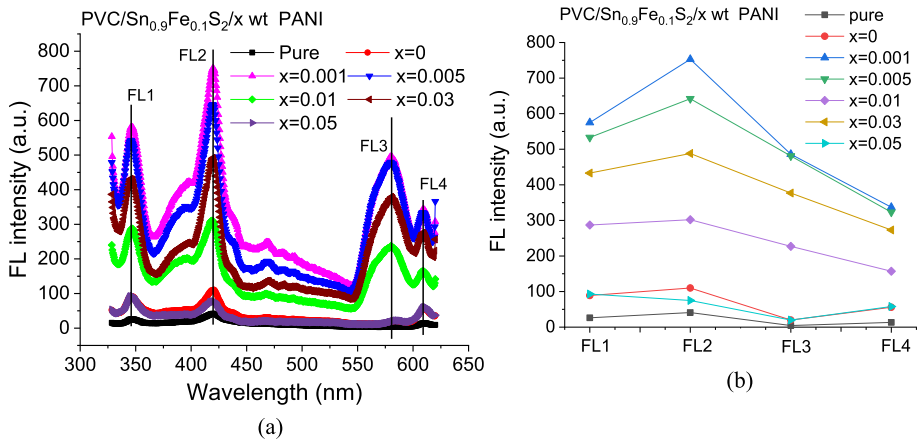


Fig. 11 **a** FL spectra and **b** changing of the FL sub peaks for PVC, PVC/Sn_{0.9}Fe_{0.1}S₂ and PVC/Sn_{0.9}Fe_{0.1}S₂/x wt% PANI polymers

3.4 DC electrical conductivity

Figure 12 shows the variation of $\ln(\sigma)$ with the inverted temperature ($1000/T$) for PVC, PVC/Sn_{0.9}Fe_{0.1}S₂ and PVC/Sn_{0.9}Fe_{0.1}S₂/x wt% PANI polymers. As depicted in the graph, the $\ln(\sigma)$ values for all polymers decreased as the inverted temperature ($1000/T$) increased. Also, the dc conductivity was reduced depending on the amount of filler, dispersion, and polymer-filler interaction (Ramazanov et al. 2020).

The dc conductivity of the polymer as a function of temperature can be described using the Arrhenius relation (Ramazanov et al. 2020):

$$\sigma_{dc} = A \exp(-E_A/k_B T) \tag{3}$$

Fig. 12 Variation of $\ln\sigma$ with temperature for PVC, PVC/Sn_{0.9}Fe_{0.1}S₂ and PVC/Sn_{0.9}Fe_{0.1}S₂/x wt% PANI polymers

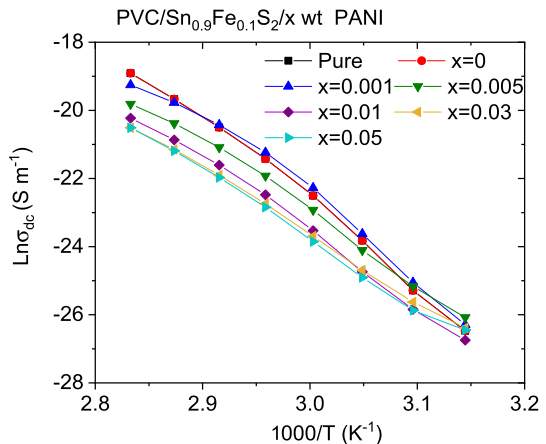


Table 1 Activation energy for PVC, PVC/Sn_{0.9}Fe_{0.1}S₂ and PVC/Sn_{0.9}Fe_{0.1}S₂/x wt% PANI polymers

Polymer	E_A (eV)
Pure	0.213
$x=0$	0.206
$x=0.001$	0.239
$x=0.005$	0.179
$x=0.01$	0.187
$x=0.03$	0.168
$x=0.05$	0.172

where E_A , A and k_B are the dc conductivity activation energy, temperature independent constant (based on the physical and chemical properties of the polymers) and Boltzman's constant, respectively.

The value of E_A for different polymers can be determined after performing the least squares fitting of the dc data using the last formula, Table 1. It can be noticed that E_A of PVC (0.213 eV) decreased to 0.206 eV as it loaded with Sn_{0.9}Fe_{0.1}S₂. Upon loading PVC/Sn_{0.9}Fe_{0.1}S₂ polymer with different contents of PANI, E_A decreased in general, except in the sample with 0.001 wt % PANI, it increased to 0.239 eV. The lowest E_A (0.168 eV) value can be obtained as PANI becomes 0.03 wt%. This result may be caused by the variation of the delocalized charge carriers in different samples (Taha 2018).

4 Conclusion

Sn_{0.9}Fe_{0.1}S₂ has a single phase of hexagonal brucite structure with highly anisotropic crystallite size and microstrain. All patterns disclosed the same characteristics as pure PVC pattern with a poor crystallization. EDS analysis confirmed the doping of PVC by Sn_{0.9}Fe_{0.1}S₂ and/or PANI. The surface morphology of PVC film turns to rough as it doped with Sn_{0.9}Fe_{0.1}S₂ and/or PANI. The n value has its maximum value as PVC/Sn_{0.9}Fe_{0.1}S₂ doped with 0.001 wt % PANI. In the visible range, sample with $x=0.001$ has a higher ϵ' value while sample with $x=0.05$ has a higher ϵ'' , VELF and SELF values. The value of σ_{opt} and NLO parameters for PVC polymer was increased as it loaded with Sn_{0.9}Fe_{0.1}S₂ and increased further as it was doped with different amounts of PANI. All polymers emitted UV, blue, yellow, and orange colors and their intensity was affected by the ratio of PANI. The dc conductivity and activation energy in general were reduced as the amount of PANI increased. PVC/Sn_{0.9}Fe_{0.1}S₂ with PANI above $x=0.001$ wt% has a good UVA absorbance. Samples with $x=0.005$ and 0.01 exhibited a band pass filter for laser protection. The reduction in optical band gap nominated doped polymers to be used in solar cells, photocatalysis and optoelectronic applications. The improvement in the values of n enables the doped polymers to be suggested as antireflection coatings for solar cells, photonic crystals, and Bragg gratings. The development in the NLO of doped PVC with Sn_{0.9}Fe_{0.1}S₂ and/or PANI is considered a helpful guide for upcoming optoelectronic applications.

Acknowledgements The authors extend their appreciation to the Deputyship for Research & Innovation, Ministry of Education in Saudi Arabia for funding this research. (IFKSURC-1-1004)

Author contributions All authors have contributed, discussed the results and approved the final manuscript.

Funding This work is supported by Deputyship for Research & Innovation, Ministry of Education in Saudi Arabia.

Data availability The authors confirm that the data supporting the findings of this study are available within the article.

Declarations

Conflict of interest The authors declare that they have no conflict of interest.

Ethical approval We agreed all terms and conditions for Ethics approval.

References

- Abdel-Fattah, E., Alharthi, A.I., Fahmy, T.: Spectroscopic, optical and thermal characterization of polyvinyl chloride-based plasma-functionalized MWCNTs composite thin films. *Appl. Phys. a* **125**, 475 (2019)
- Abdelhamied, M.M., Atta, A., Abdelreheem, A.M., Farag, A.T.M., El Okr, M.M.: Synthesis and optical properties of PVA/PANI/Ag nanocomposite films synthesis and optical properties of PVA/PANI/Ag nanocomposite films. *J. Mater. Sci. Mater. Electron.* **31**, 22629–22641 (2020)
- Abed, R.N., Yousif, E., Abed, A.R.N., Rashad, A.A.: Synthesis thin films of poly (Vinyl Chloride) doped by aromatic organosilicon to absorb the incident light. *Silicon* **14**, 11829–11845 (2022)
- Ahmad, A.A., Bani-Salameh, A.A., Al-Bataineh, Q.M., Jum'h, I., Telfah, A.D.: Optical, structural and morphological properties of synthesized PANI-CSA-PEO-based GaN nanocomposite films for optoelectronic applications. *Polym. Bull.* **80**, 809 (2023)
- Ahmed, R.M., Atta, M.M., Taha, E.O.: Optical spectroscopy, thermal analysis, and dynamic mechanical properties of graphene nano-platelets reinforced polyvinylchloride. *J. Mater. Sci. Mater. Electron.* **32**, 22699–22717 (2021)
- Biswas, M.R.U.D., Ho, B.S., Oh, W.-C.: Eco-friendly conductive polymer-based nanocomposites, BiVO₄/graphene oxide/polyaniline for excellent photocatalytic performance. *Polym. Bull.* **77**, 4381 (2020)
- Brunner, A.J.: X-ray diffraction pattern of poly (vinyl chloride). *Polym. Lett.* **10**, 379–383 (1972)
- Chen, J., Nie, X.A., Jiang, J.C., Zhou, Y.H.: Thermal degradation and plasticizing mechanism of poly(vinyl chloride) plasticized with a novel cardanol derived plasticizer. *IOP Conf. Ser. Mater. Sci. Eng.* **292**, 01200 (2017)
- Chen, Y., Wang, T., Pan, J., Wang, M., Chen, A., Chen, Y.: Fabrication, characterization and photocatalytic degradation activity of PS/PANI/CeO₂ tri-layer nanostructured hybrids. *Bull. Mater. Sci.* **45**, 45 (2022). <https://doi.org/10.1007/s12034-021-02635-8>
- El-Hachemi, B., Miloud, S., Sabah, M., Souad, T., Zineddine, O., Boubekour, B., Toufik, S.M., Ouahiba, H.: Structural, electrical and optical properties of PVC/ZnTe nanocomposite. *J. Inorg. Organomet. Polym.* **31**, 3637–3648 (2021a)
- El-Hachemi, B., Miloud, S., Sabah, M., Souad, T., Zineddine, O., Boubekour, B., Toufik, S.M.: Halimi, Ouahiba, structural, electrical and optical properties of PVC/ZnTe nanocomposite. *J. Inorg. Organomet. Polym.* **31**, 3637–3648 (2021b)
- El-Naggar, A.M., Heiba, Z.K., Mohamed, M.B., Kamal, A.M., Osman, M.M., Albassam, A.A., Lakshminarayana, G.: Embedding of 50%PVA/50%PVP blend with Sn_{0.75}Mo_{0.25}S₂ (M = Y, Fe, Cr, V); structural and optical study. *Appl. Phys. A* **127**, 1–7 (2021)
- El-naggar, A.M., Heiba, Z.K., Mohamed, M.B., Kamal, A.M., Osman, M.M., Albassam, A.A., Lakshminarayana, G.: Improvement of the optical characteristics of PVA/PVP blend with different concentrations of SnS₂/Fe. *J. Vinyl Addit. Technol.* **28**(1), 82–93 (2022a)
- El-naggar, A.M., Heiba, Z.K., Mohamed, M.B., Kamal, A.M., Lakshminarayana, G.: M ASHar, Structural, linear and nonlinear optical properties of poly (vinyl alcohol)(PVA)/polyethylene glycol (PEG)/SnS₂: Y nanocomposite films. *Optik* **258**, 168941 (2022b)
- El-naggar, A.M., Alsaggaf, A., Heiba, Z.K., Kamal, A.M., Aldhafiri, A.M., Fatehmulla, A., Mohamed, M.B.: Exploring the structural, optical and electrical characteristics of PVA/PANi blends. *Opt. Mater.* **139**, 113771 (2023)

- El-naggar, A.M., Heiba, Z.K., Kamal, A.M., Mohamed, M.B.: The role of cobalt amount in ZnCdS nanofiller on the optical, thermal, dielectric and structure properties of PVA/PVP/PEG blends. *Opt. Quant. Electron.* **55**(7), 609 (2023b)
- Gaabou, L.H.: Effect of addition of TiO₂ nanoparticles on structural and dielectric properties of polystyrene/polyvinyl chloride polymer blend. *AIP Adv.* **11**(10), 105120 (2021)
- Graeme, A.G.: Characterization of solid polymers by luminescence techniques. *Pure. Appl. Chem.* **57**(7), 945–954 (1985)
- Harshvardhan, P Yadav, Singh, B.: Systematic investigation of the effect of SnS₂ nanofiller content on the piezoelectric performance of the PVDF-TrFE-based nanogenerator. *Mater. Today Proc.* (2023). <https://doi.org/10.1016/j.matpr.2023.05.607>
- Jia, P., Zhang, M., Hu, L., Wang, R., Sun, C., Zhou, Y.: Cardanol groups grafted on poly(vinyl chloride)—synthesis. *Perform. Plasticization Mech. Polym.* **9**, 621 (2017)
- Kroschwitz, I.: *Electronic Properties of Polymers*. Wiley, Hoboken (1988)
- Laurari, I., Lakhari, N., Belgherbi, O., Medjili, C., Berkani, M., Vassehgan, Y., Golzadeh, N., Lakhdari, D.: Antimicrobial and antifungal properties of NiCu-PANI/PVA quaternary nanocomposite synthesized by chemical oxidative polymerization of polyaniline. *Chemosphere* **291**, 132696 (2022)
- Makled, M.H., Sheha, E., Shanap, T.S., El-Mansy, M.K.: Electrical conduction and dielectric relaxation in p-type PVA/CuI polymer composite. *J. Adv. Res.* **4**, 531–538 (2013)
- Mallakpour, S., Sadaty, M.A.: Thiamine hydrochloride (vitamin B1) as modifier agent for TiO₂ nanoparticles and the optical, mechanical, and thermal properties of poly(vinyl chloride) composite films. *RSC Adv* **6**, 92596–92604 (2016)
- Mallakpour, S., Shamsaddinimotlagh, S.: Ultrasonic-promoted rapid preparation of PVC/TiO₂-BSA nanocomposites: characterization and photocatalytic degradation of methylene blue. *Ultrason. Sonochem.* **41**, 361–374 (2018)
- Mansour, A.F., Elfalaky, A., Abdel Maged, F.: Synthesis, characterization and optical properties of PANI/PVA Blends. *IOSR J. Appl. Phys. (IOSR-JAP)* **7**(4), 37–45 (2015)
- Mirmohseni, A., Wallace, G.G.: Preparation and characterization of processable electroactive polyaniline–polyvinyl alcohol composite. *Polymer* **44**, 3523–3528 (2003)
- Mohamed, M.B., Heiba, Z.K.: Structural and properties correlation in PANI–Mo doped CoFe₂O₄ nanocomposite. *J. Mater. Sci. Mater. Electron.* **28**(23), 17578–17586 (2017)
- Rajendran, S., Sivakumar, P., Babu, R.S.: Studies on the salt concentration of a PVdF–PVC based polymer blend electrolyte. *J. Power Source* **164**, 815–821 (2007)
- Ramazanov, M.A., Rahimli, A.M., Hajiyeva, F.V.: The influence of titanium dioxide (TiO₂) nanoparticles on the structure, optical and dielectric properties of polyvinyl chloride (PVC). *Mod. Phys. Lett. B* **34**(28), 2050310 (2020)
- Rouabah, N., Boudine, B., Nazir, R., Zaatat, M., Sebais, M., Halimi, O., Soltani, M.T., Chala, A.: Structural, optical and photocatalytic properties of PVC/CdS nanocomposites prepared by soft chemistry method. *J. Inorg. Organomet. Polym.* **31**, 1102–1110 (2021)
- Sadek, E.M., Mansour, N.A., Ahmed, S.M., Abd-El-Messieh, S.L., El-Komy, D.: Synthesis, characterization and applications of poly (vinyl chloride) nanocomposites loaded with metal oxide nanoparticles. *Polym. Bull* **78**, 5481–5502 (2021)
- Sayed, W.M., Soliman, L.I.: Optical properties of polyaniline salt and polyaniline base with KBr, Co (CH₃COO)₂ and picric acid composites. *Fizika (zagreb)* **4**, 147–152 (2000)
- Selvi, J., Mahalakshmi, S., Parthasarathy, V.: Synthesis, structural, optical, electrical and thermal studies of poly(vinyl alcohol)/CdO nanocomposite films. *J. Inorg. Organomet. Polym.* **27**, 1918–1926 (2017)
- Sharma, S., Singh, K.L., Kumar, M., Prasher, S.: Structural, optical and thermal properties of PVC/polyaniline composite thin films. *JOM* **74**(2), 1–7 (2021)
- Soman, V.V., Kelkar, D.S.: FTIR studies of doped PMMA-PVC blend system. *Macromol Symp* **277**, 152–161 (2009)
- Taha, T.A., Saleh, A.: Dynamic mechanical and optical characterization of PVC/fGO polymer nanocomposites. *Appl. Phys. A* **124**, 600 (2018)
- Taha, T.A., Hendawy, N., El-Rabaie, S., Esmat, A., El-Mansy, M.K.: Effect of NiO NPs doping on the structure and optical properties of PVC polymer films. *Polym. Bull* **76**, 4769–4784 (2019)
- Taha, T.A., Hendawy, N., El-Rabaie, S., Esmat, A., El-Mansy, M.K.: Fluorescence and dielectric spectroscopy identification of polyvinyl chloride/NiO nanocomposites. *J. Mol. Struct.* **1212**, 128162 (2020)
- Tao, S., Zhu, S., Feng, T., Zheng, C., Yang, B.: Crosslink-enhanced emission effect on luminescence in polymers: advances and perspectives. *Angew. Chem. Int. Ed.* **59**, 9826–9840 (2020)
- Tauc, J.: Optical properties and electronic structure of amorphous Ge and Si. *Mater. Res. Bull.* **3**(1), 37–46 (1968)

- Wadatar, N.S., Waghuley, S.A.: Characterizing the electro-optical properties of polyaniline/poly(vinyl acetate) composite films as-synthesized through chemical route. *Results Surf. Interfaces* **4**, 100016 (2021)
- Wang, B., Jiang, F., Ma, X., Dong, Z., Liu, Y.: Preparation of highly dispersed ZnO nanoparticles to fabricate ultraviolet-shielding poly(vinyl chloride) films. *Colloid Polym. Sci.* **300**, 51–57 (2022)
- Wu, C., Wicks, D.A.: Use of fluorescence for the high-throughput evaluation of synergistic thermal and photo stabilizer interactions in poly (vinyl chloride). *Rev. Sci. Instrum* **76**, 062212 (2005)
- Yazid, M.I.B.M., Ghani, S.A., Jin, T.S., Osman, A.F., Mohd Din, S.H.: Utilization of polyaniline (PAni) as conductive filler on poly (Ethylene Oxide)/poly (Vinyl Chloride) films: effects of naphthalene as surface modifier on electrical conductivity. *J. Phys. Conf. Ser.* **908**, 012006 (2017)

Publisher's Note Springer Nature remains neutral with regard to jurisdictional claims in published maps and institutional affiliations.

Springer Nature or its licensor (e.g. a society or other partner) holds exclusive rights to this article under a publishing agreement with the author(s) or other rightsholder(s); author self-archiving of the accepted manuscript version of this article is solely governed by the terms of such publishing agreement and applicable law.